# Formation Control of a Drifting Group of Marine Robotic Vehicles

Nicholas R. Rypkema and Henrik Schmidt

**Abstract** This paper presents a comparative study into three strategies for formation control of autonomous underwater/surface vehicles (AUVs/ASVs) in the presence of ocean or river currents. Deploying multiple AUVs in formation would provide large-scale spatial and temporal data for oceanographic research. However, multi-AUV formation control is difficult because of the communication and navigation constraints of the underwater environment. The strategies we developed to address these challenges are distributed, use relative positions of neighboring vehicles to coordinate, and leverage current to increase endurance. We present simulation results for a group of 20 AUVs operating in 4D ocean currents, and compare control strategies in terms of energy expenditure and formation quality. We validated the most promising strategy with real robot experiments using three ASVs on the Charles River, and provide an initial analysis of the data.

## 1 Introduction

Advances in autonomous underwater vehicle (AUV) technology have led to their wide-spread acceptance and adoption in scientific, commercial, and defense applications. At the same time, research progress in coordination and control of multi-robot systems has led to their effective deployment in the field. Applying multi-robot control concepts on AUVs would improve efficacy in missions such as tracking oceanographic processes and localizing acoustic sources, and could open up additional applications such as seismic surveying using multiple AUVs as an acoustic receiver array. Some existing missions that would be well served by multi-AUV sampling include monitoring ocean temperature, tracking algal blooms, and map-

Nicholas R. Rypkema
Massachusetts Institute of Technology, Cambridge, MA, USA, e-mail: rypkema@mit.edu

Henrik Schmidt
Massachusetts Institute of Technology, Cambridge, MA, USA, e-mail: henrik@mit.edu

ping hazardous chemical spills. However, existing multi-robot control strategies do not take into account the unique constraints posed by AUV operations in the undersea environment; algorithms must be distributed, robust to localization error, and operable with minimal inter-vehicle communication.

We are interested in a particular multi-robot control task, known as formation control, in which a group of vehicles coordinate to establish and maintain a desired geometric pattern. Various approaches for distributed formation control have been described in previous literature, including physics-based approaches [1, 2, 3, 4], leader-follower methods [5, 6], potential-field approaches [7, 8], and virtual structure methods [9, 10, 11]. Early experimental work in underwater vehicle formation control includes the use of artificial attraction/repulsion potentials to maintain a triangular shape for three Slocum gliders [12], as well as a leader-follower method in which a simple proportional controller is used to maintain distance/velocity relative to a leading AUV [13]. More recent work [14] describes a similar leader-follower approach, in which acoustic modems mounted on three autonomous surface vehicles (ASVs) are used to determine range from a single follower to two leaders; a proportional-integral controller operating on the follower uses these ranges to maintain velocity and heading relative to the leaders to maintain a triangular formation.

The primary goal of this work is the development of formation control strategies allowing a group of AUVs to form and maintain a hexagonal lattice in the presence of ocean currents. Unlike previous work, we wish to utilize the prevailing current to power the overall movement of the formation, with the vehicles only using their motors to maintain the desired geometry. We describe three behavior-based algorithms for AUVs, each of which is distributed and leaderless. Each vehicle performs formation control using relative range and bearing measurements to its neighbors within a specified radius, and does so by using these measurements to continuously calculate a vehicle target position. This is in contrast to previous approaches, in which control policies for vehicle speed and heading are explicitly derived so as to minimize error in formation position relative to leader vehicles. By specifying target positions that we wish our vehicles to track, our approach allows us to abstract away the lower-level control layers. This approach is extremely flexible and can effortlessly combine range/bearing information from an arbitrary number of neighbors, building formations that are large and leaderless. Multiple behaviors can also be combined into more complex behaviors. The cost of this flexibility is the inability to provide formal guarantees on formation convergence. In this paper, we compare the performance of three newly developed algorithms in simulation, and provide results from validating the most promising strategy in field experiments with three ASVs.

## 2 Formation Control Algorithms

In our approach, vehicles operate under a frontseat/backseat paradigm, in which the backseat is responsible for performing calculations for formation control, communications and autonomy using MOOS-IvP [15], a software architecture for vehicle

autonomy. The backseat sends desired heading, depth and speed commands to the frontseat, which executes basic control and navigation.

Our formation control algorithms operate by outputting a target position which represents the optimal vehicle location to maintain formation. Each control strategy is built upon a common target behavior which sends desired heading and speed commands to the frontseat, illustrated in figure 1. This behavior operates as follows: It begins by directing the vehicle at a heading towards the target with maximum speed. Speed is linearly decreased within a specified drifting radius, and set to zero upon location arrival (either by entering the capture radius, or if there is lack of progress within the slip radius). The vehicle is then left to drift freely until it exits the drifting radius.

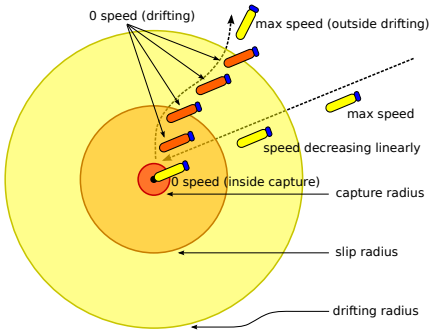


**Fig. 1:** Illustration of the target behaviour, which directs the vehicle to a target point and then leaves it to drift within a drifting radius.

The target behavior is used by vehicles to exploit the prevailing current for propulsion during times in which they are free to drift. We can trade-off formation accuracy against energy consumption by changing the drifting radius.

## *2.1 Attraction/Repulsion Formation Control:*

Inspired by the simplicity of physics-based approaches, our first algorithm performs formation control through the use of artificial attraction/repulsion potentials. We define our potential as:

$$f(r) = \left(\frac{s^3}{2 \cdot r^2}\right) + (r - 3 \cdot s) \tag{1}$$

This potential is placed at the positions of two neighboring vehicles, with $s$ being the desired distance from, and $r$ the range to, each neighbor. The first neighbor is the nearest neighbor, and the second is chosen such that the sum of edge lengths of the triangle created by the three vehicles is minimal. Equation 2 shows the minimization of equation 1 over two dimensions (where $N_s$ contains the positions of the two neighbors). Solving this equation yields a minimum $(x^*, y^*)$ representing the target position for the vehicle, which occurs at a distance $s$ from both neighbors.

$$(x^*, y^*) = \underset{(x,y)}{\operatorname{argmin}} \sum_{(x_i,y_i) \in N_s} \left(\frac{s^3}{2 \cdot \left(\sqrt{(x - x_i)^2 + (y - y_i)^2}\right)^2}\right) + \left(\left(\sqrt{(x - x_i)^2 + (y - y_i)^2}\right) - 3 \cdot s\right) \tag{2}$$

This algorithm can only produce a hexagonal lattice formation, but has the advantage of only requiring the relative positions of neighbors to operate. Unfortunately, these formations are prone to breaking apart in ocean currents.

## 2.2 Pairwise Trigonometric Formation Control:

In our second formation control algorithm, each vehicle is given a unique ID and a user-defined plan specifying its desired position within the formation. Given this plan and the IDs of neighbors within the vehicle's communication radius, the algorithm calculates the relative distance $D_d$ and angle $\phi_d$ from the midpoint between any pair of neighbors $i, j$ to the desired position of the vehicle (where $(x_{i_p}, y_{i_p})$ and $(x_{j_p}, y_{j_p})$ are the plan-specified positions of the neighbors relative to the vehicle):

$$D_d = \sqrt{((x_{i_p} + x_{j_p})/2)^2 + ((y_{i_p} + y_{j_p})/2)^2} \tag{3}$$

$$\phi_d = atan2((y_{i_p} + y_{j_p})/2, (x_{i_p} + x_{j_p})/2) - atan2(y_{j_p} - y_{i_p}, x_{j_p} - x_{i_p}) \tag{4}$$

This plan-calculated distance and angle are then used to determine a position using the actual relative positions of these two neighbors $(x_i, y_i)$ and $(x_j, y_j)$:

$$(x^*_{ij}, y^*_{ij}) = ((x_i + x_j)/2, (y_i + y_j)/2) + (D_d \sin\phi_d, D_d \cos\phi_d) \tag{5}$$

The position $(x^*_{ij}, y^*_{ij})$ is essentially a 'vote' by this neighbor pair of where the target for the vehicle should be. The combined target position $(x^*, y^*)$ is calculated as the centroid of all votes from every possible unique neighbor pair combination seen by the vehicle. This control strategy is visualized in figure 2.

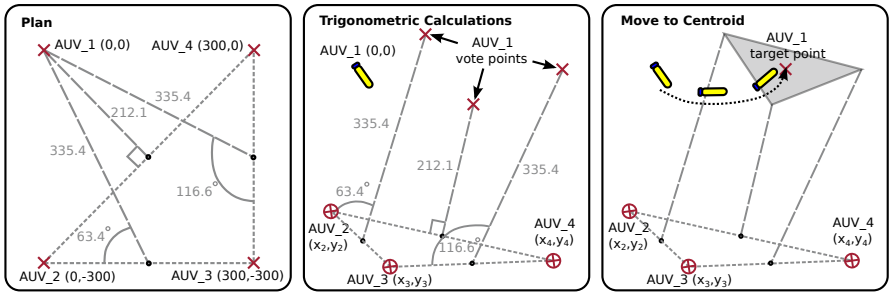


**(a)** Use plan to calculate distances and angles from midpoint between pairs of neighbors to desired vehicle position

**(b)** Apply plan-calculated distances and angles to corresponding midpoints of actual neighbor pairs

**(c)** Calculate vehicle target position $(x^*, y^*)$ as centroid of votes $(x^*_{ij}, y^*_{ij})$ from all neighbor pair combinations

**Fig. 2:** Illustration of the pairwise trigonometric formation control strategy.

## 2.3 Point Set Registration Formation Control:

Our third formation control algorithm follows from the previous in that it also requires each vehicle to have a unique ID and a corresponding position in a user-defined plan. Since a vehicle is able to detect the IDs of neighbors within its com-

munications radius, it can look up their corresponding positions in the plan. All that remains to be done is to calculate the rigid transformation that optimally aligns desired neighbor positions to actual neighbor positions, a process broadly termed as point set registration. Unlike the previous algorithm, in which votes from neighbor pairs are used to calculate the target position, this strategy essentially treats the entire plan as a rigid structure, and transforms it to best align with neighbor positions.

Given the set of relative positions of neighbors within the vehicle's communications radius $\{(x_0,y_0)=(0,0),(x_1,y_1),...,(x_n,y_n)\}$, and their corresponding relative positions defined in the plan $\{(x_{0_p},y_{0_p})=(0,0),(x_{1_p},y_{1_p}),...,(x_{n_p},y_{n_p})\}$ (we include the vehicle's own position as $(0,0)$ in both sets), the optimal rigid transformation between the two point-sets is given by:

$$(R,\mathbf{t}) = \underset{R,\mathbf{t}}{\operatorname{argmin}} \sum_{i=0}^{n} ||(R\begin{bmatrix} x_{i_p} \\ y_{i_p} \end{bmatrix} + \mathbf{t}) - \begin{bmatrix} x_i \\ y_i \end{bmatrix}||^2 \tag{6}$$

A closed form solution of this minimization is performed as in [16], resulting in an optimal rotation matrix, $R$, and translation vector, $\mathbf{t}$, which is applied to the vector of plan positions. As a result, a target position $(x^*,y^*)$ for the vehicle is generated as the first point of this transformed vector. Figure 3 illustrates this algorithm.

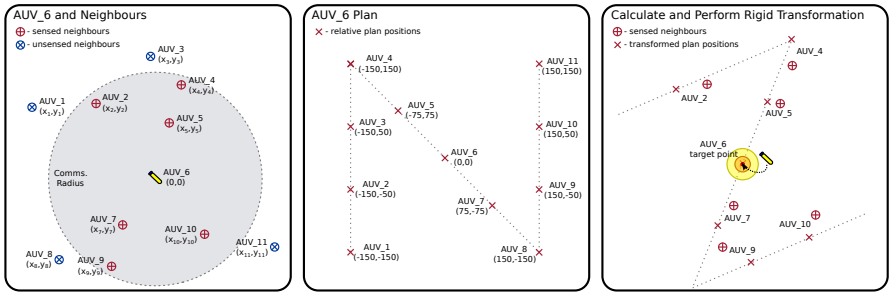


**(a)** AUV_6 receives pings containing IDs and relative positions of neighbors within its communication radius

**(b)** AUV_6 uses its plan to obtain planned relative positions of neighbors it has sensed

**(c)** AUV_6 applies a rigid transformation to planned positions, and as a result the plan is optimally aligned to actual neighbor positions

**Fig. 3:** Illustration of the point set registration formation control strategy.

As with the pairwise trigonometric algorithm, this strategy can create formations of arbitrary shape, with the disadvantage of having to communicate vehicle IDs.

## 3 Experimental Setup

Experiments were performed both in simulation and in the field, to investigate the qualities of our three formation control algorithms. Performance of each algorithm was quantified using two measures. The first is a metric reflecting the formation

quality, in which the distance between each pair of neighboring vehicles is averaged over the number of pairs, and compared to the desired inter-vehicle distance. Past literature has typically used this measure to quantify control strategy effectiveness. The second is a simplified measure of average energy expenditure, in which power consumption is calculated as the sum of three factors: integrated power consumption due to motor propulsion (which only occurs when vehicles are thrusting), integrated power consumption due to hotel load, and power consumption due to acoustic pings.

Simulations were performed in the Laboratory for Autonomous Marine Sensing Systems (LAMSS) MOOS-IvP Ocean Simulation environment. This environment includes vehicle dynamics and acoustic communications, as well as physics-driven simulation of 3D time-varying oceanographic environments via MSEAS ocean models [17]. Vehicle dynamics were based on a simplified model of the Folaga AUV [18], a vehicle that has active depth and turn-in place control. We assumed that each vehicle was able to measure relative range, bearing and ID to neighbors within a radius of 550 m, with Gaussian noise with standard deviation $5^\circ$ in bearing and 1.5 m in range, through the use of acoustic pings transmitted by each vehicle every 30 s. The target drifting radius was set to 20 m. We performed simulation experiments using 20 AUVs, whose positions were randomly initialized within a $200 \times 200$ m box. The group was instructed to construct a hexagonal lattice with a desired separation distance of 300 m, and was left to drift freely in ocean currents for approximately 5 hours in simulation time.

to investigate the validity of our approach, field experiments were run with three Kingfisher ASVs. Each vehicle has a thruster in each pontoon, an IMU, compass and GPS, and has a MOOS-IvP interface to receive heading and speed commands. Commands were sent from a Raspberry Pi 2 payload computer, with our MOOS-IvP architecture running the point set registration formation control strategy. Since we did not have the hardware to detect range and bearing between vehicles, vehicle state was transmitted via 802.11 WiFi to a shoreside computer which simulated acoustic communications. Range/bearing/ID information was then transmitted back to the vehicles. Due to the limited size of the operations area (approximately $500 \times 350$ m), we selected a desired separation distance of 60 m, a drifting radius of 6 m, and a ping period of 20 s; we also halved the Gaussian standard deviations for simulated bearing and range measurements to $2.5^\circ$ and 0.75 m respectively. The three vehicles were directed upstream, instructed to form an equilateral triangle, and left to drift downstream in formation.

**Fig. 4:** Kingfisher ASVs used for field experiments.

## 4 Simulation Results

Simulation trials were performed for each formation control algorithm. Vehicle positions were initialized randomly in a $200 \times 200$ m area. They then constructed a hexagonal formation (and in the case of pairwise trigonometric and point set registration algorithms, each vehicle was given a formation plan for a $4 \times 5$ hexagonal lattice), and freely drifted in ocean currents modeled using an MSEAS model of the Red Sea. Typical vehicle trajectories for these simulations are shown in figure 5.

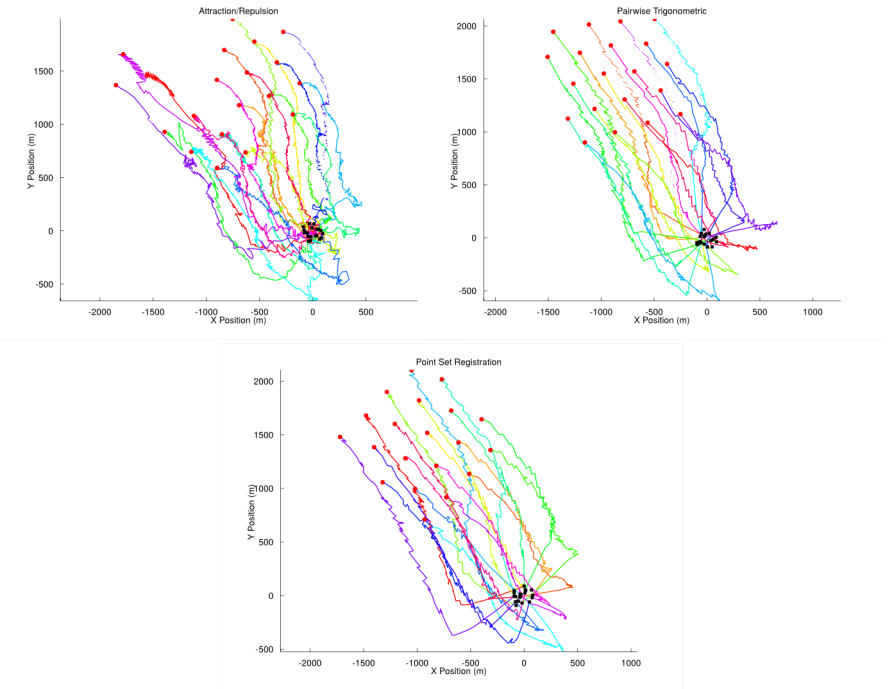


**Fig. 5:** Simulated trajectories of 20 AUVs for attraction/repulsion (top left), pairwise trigonometric (top right), and point set registration (bottom) formation control strategies. AUVs are randomly deployed in a $200 \times 200$ m area, construct a hexagonal formation, and drift in formation for 16000 s, exploiting ocean currents for propulsion.

Qualitative examination of the three algorithms indicate that although our attraction/repulsion strategy was able to construct the desired hexagonal lattice, the group eventually broke apart into three smaller groups while drifting, a consequence of continuous disturbances caused by ocean currents. Past literature concerning physics-based formation control typically demonstrated formation control in environments free of disturbances, or with few vehicles; we show here that such approaches may not be robust in disturbance-rich domains. In addition, we see that the trajectories are quite chaotic because the artificial potentials push and pull on different vehicles. These issues are partly a consequence of the fact that this algorithm only makes use of two neighbors for control. Two-neighbor control was used to

achieve the desired inter-vehicle distance; summation of potentials from additional neighbors causes the minimum (and thus the target) to shift. The formation tends to break apart when a subgroup of vehicles all select neighbors amongst themselves and the currents pull in different directions.

In contrast, both the pairwise trigonometric and point set registration strategies were able to efficiently construct and maintain the desired $4 \times 5$ hexagonal lattice formation, with the group using ocean currents to propel itself almost 1.8 km in 5 hours. Global knowledge in the form of the user-defined formation plan has enabled each vehicle to maintain its relative position in the group, even as the group freely rotated while drifting. Vehicle trajectories possess a characteristic sawtooth movement, as vehicles alternated between drifting while in the drifting radius, and thrusting back to target.

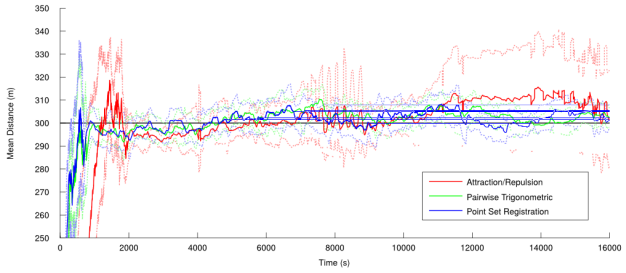


**Fig. 6:** Results of simulation - mean distance between vehicles in the formation; dashed lines indicate standard deviation. Experiments were conducted with 20 AUVs. AUVs regulate distance using user-specified distance and have access to relative neighbor positions and IDs within comms. radius once every 30 s.

Figure 6 illustrates the mean distance between neighboring pairs of vehicles, along with envelopes of standard deviation. This provides a measure of formation quality. Our qualitative observations of the attraction/repulsion algorithm are clearly reflected by the standard deviation envelopes of this measure. Formation break-up first occurs at about 7000 s, causing oscillatory movement that culminates in two distinct vehicle subgroups. A second break-up episode slowly unfolds starting at around 11000 s, causing the metric to diverge from the desired separation distance and three subgroups to emerge by the end of the mission.

Examining the formation quality metric for the pairwise trigonometric and point set registration algorithms, we see that both perform similarly. Both strategies are able to construct the formation to the desired separation distance within 1000 s. Their standard deviation envelopes are well within the set 20 m target drifting radius throughout the mission, reflecting the fact that the hexagonal lattice formation is consistently maintained to the desired accuracy.

Figure 7 illustrates vehicle mean energy expenditure with envelopes of standard deviation. Unsurprisingly, the attraction/repulsion strategy consumes the greatest amount of energy, as the artificial potentials cause vehicles to continuously jostle with their neighbors. The standard deviation envelopes demonstrate that the point set registration strategy makes use of energy more consistently across all vehicles

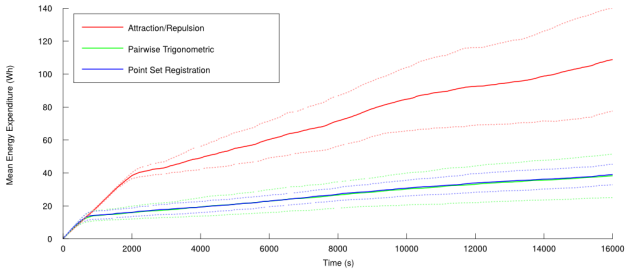


**Fig. 7:** Results of simulation - mean vehicle energy expenditure; dashed lines indicate standard deviation. Experiments were conducted with 20 AUVs. Expenditure is sum of integrated motor power consumption, hotel power consumption and acoustic transmission power consumption.

than the pairwise trigonometric algorithm, though both have similar mean energy expenditures. The rate of energy expenditure is significantly lower once the formation has been constructed and is free to drift. These results suggest that if the prevailing current is known and along the desired trajectory, ocean current could be leveraged for formation propulsion for long-term sampling using groups of vehicles.

## 5 Experimental Results

Field experiments were performed using three Kingfisher ASVs on a portion of the Charles River by the MIT Sailing Pavilion. Vehicle state was monitored on a shoreside computer, which also performed simulation of acoustic communications. The ASVs were manually directed upriver, instructed to form an equilateral triangle and left to drift downriver. Leader-following was then performed by manually directing a single vehicle upstream, causing the remaining two ASVs to naturally follow in an attempt to maintain formation. Finally, three simulated ASVs were added, easily allowing us to construct a larger equilateral triangle using three simulated and three real ASVs. All vehicles ran the point set registration algorithm in a distributed fashion. Trajectories of the ASVs during different phases are illustrated in figure 8.

The point set registration formation control strategy was successfully able to construct the desired triangle and maintain that formation as the group drifted downriver (figure 8 (a)-(c)). Unlike the simulated vehicles the Kingfisher ASVs are not able to rotate in-place, but our target-based formation control strategy was still able to construct the desired formation. This highlights an advantage of our approach: formation control is achieved without needing to know exact vehicle dynamics.

The ability to perform leader-following was a natural consequence of our formation control algorithm using only three vehicles. Figure 8 (d)-(f) shows this behavior: the rightmost ASV is manually directed upstream, and the remaining two vehicles follow in an effort to maintain formation. However, due to the 20 s interval between simulated acoustic pings, the followers lag the leader and are unable to continuously maintain a perfect triangle formation.

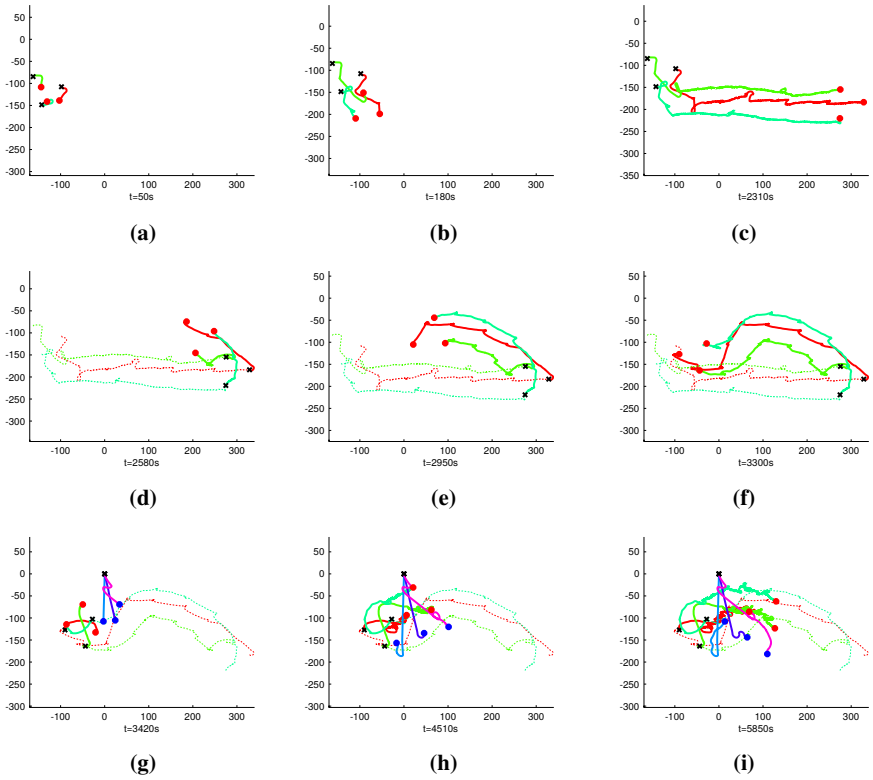


**Fig. 8:** Results of field experiments. (a)-(c): Trajectories of three Kingfisher ASVs establishing formation and drifting East on the Charles River. (d)-(f): Trajectories of the three Kingfisher ASVs leader-following in formation, with operator-driven ASV at forward corner of triangle (red line trajectory). (g)-(i): Trajectories of actual Kingfisher ASVs (red) and simulated ASVs (blue) when three simulated ASVs are added and a larger formation is constructed and left to drift freely.

Figure 8 (g)-(i) illustrate group reformation when three simulated ASVs (blue) were added to the group. Both real and simulated vehicles can interact using the MOOS-IvP architecture. Like in the original three-vehicle case, the algorithm was able to construct the desired triangular formation. Since river currents were not simulated for the virtual vehicles, the real vehicles (red) tended to frequently reposition themselves. This caused the group to rotate, as is visible in figure 8 (h)-(i).

Figure 9 depicts the average distance between neighboring pairs of vehicles. The three phases of the experiment are clearly visible in this measurement, reflecting the quality of the formation. The first phase (figure 8 (a)-(c)) occurred between 0 s and 2310 s, and is reflected by a mean distance metric centered around 60 m with a standard deviation of about 4 m. The effect of the target drifting radius is clearly seen in the behavior of the metric, as it repeatedly diverges from and returns to the 60 m separation distance. The leader-following second phase (figures 8 (d)-(f)) occurred between 2310 s and 3300 s, and is characterized by oscillations in the mean distance.

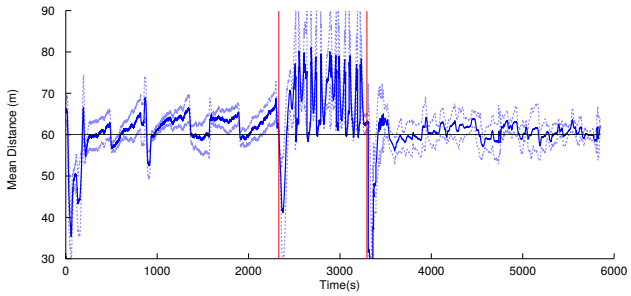


**Fig. 9:** Results of field experiments - mean distance between vehicles in the formation; dashed lines indicate standard deviation. Experiments were conducted with three real and three virtual ASVs. ASVs have access to neighboring vehicle information every 20 s using simulated acoustic comms. Red vertical lines separate the three experiment phases seen in fig. 8 (a)-(c), (d)-(f) and (g)-(i).

This was caused by the 20 s delays between simulated acoustic pings, which resulted in lag between leader and follower movement. The leader vehicle was directed in steps to give the following vehicles time to reform, resulting in these oscillations. The third stage (figures 8 (g)-(i)) occured between 3300 s and 5850 s when three virtual ASVs were introduced to the formation. This resulted in the mean distance metric dropping to 0 m upon vehicle introduction, and then settling again to center around 60 m once the larger formation was constructed. Interestingly, the addition of these vehicles caused the formation to more closely track the desired separation distance. This occurred because the simulated vehicles were not subject to external disturbances and because averaging over more vehicles stabilizes the metric.

## 6 Conclusions

We developed three algorithms for the control of a formation of autonomous underwater/surface vehicles in the presence of ocean and river currents. These algorithms are distributed, use low communication (where only range, bearing, and vehicle ID are needed once every $20-30$ s), and exploit prevailing current for group propulsion. They were compared in simulation using formation quality and energy expenditure metrics, and it was demonstrated that two of these strategies performed well in maintaining a user-defined hexagonal formation. Simulation results suggest that exploiting ocean currents could be an advantageous strategy for sampling using multiple vehicles over large areas for extended periods of time.

Field experiments using three Kingfisher ASVs demonstrated the validity of one of the formation control algorithms tested in simulation in the presence of actual river currents and simulated acoustic communications. We also demonstrated leader-follower behavior using formation control by manually directing one of the ASVs, and dynamically added virtual vehicles to show behavior utility with more vehicles and a mixture of real and simulated ASVs.

Future work will focus on replacing the simulated acoustic communications component with actual hardware. Hydrophone arrays will be used to detect range and bearing from acoustic pingers, and different acoustic waveforms will be used to transmit unique IDs. An additional direction for future research is the integration of additional behaviors with formation control, particularly behaviors for obstacle and shoreline avoidance. This could enable the deployment of an ASV formation for river sampling, allowing the group to autonomously perform water monitoring while avoiding obstacles and drifting downriver.

**Acknowledgements** The authors thank Erin Fischell for feedback and Michael Novitzky for assistance during field experiments. This material is based on work supported by APS under contract number N66001-11-C-4115 and award numbers N66001-13-C-4006 and N66001-14-C-4031.

## References

1. W. Spears, et al., *Distributed, physics-based control of swarms of vehicles*. Autonomous Robots, Volume 17, Issue 2-3, 137-162, 2004.
2. S. Prabhu, W. Li, J. McLurkin, *Hexagonal Lattice Formation in Multi-Robot Systems*. 11th International Conference on Autonomous Agents and Multiagent Systems, 2012.
3. K. Fujibayashi, et al., *Self-organizing formation algorithm for active elements*. 21st IEEE Symposium on Reliable Distributed Systems, 2002.
4. B. Shucker, J.K. Bennett, *Scalable Control of Distributed Robotic Macrosensors*. Distributed Autonomous Robotic Systems 6, Part 9, 379-388, 2007.
5. J.P. Desai, J.P. Ostrowski, V. Kumar, *Modeling and control of formations of nonholonomic mobile robots*. IEEE Transactions on Robotics and Automation, Volume 17, Issue 6, 905-908, 2001.
6. G.J. Mariottini, et al., *Leader-follower formations: uncalibrated vision-based localization and control*. IEEE International Conference on Robotics and Automation, 2403-2408, 2007.
7. R. Bachmayer, N.E. Leonard, *Vehicle networks for gradient descent in a sampled environment*. 41st IEEE Conference on Decision and Control, Volume 1, 112-117, 2002.
8. L. Chaimowicz, N. Michael, V. Kumar, *Controlling Swarms of Robots Using Interpolated Implicit Functions*. IEEE International Conference on Robotics and Automation, 2487-2492, 2005.
9. M.A. Lewis, K.H. Tan, *High Precision Formation Control of Mobile Robots Using Virtual Structures*. Journal of Autonomous Robots, Volume 4, Issue 4, 387-403, 1997.
10. C. Belta, V. Kumar, *Motion generation for formations of robots: A geometric approach*. IEEE International Conference on Robotics and Automation, Volume 2, 1245-1250, 2001.
11. M.B. Egerstedt, X. Hu, *Formation Constrained Multi-Agent Control*. IEEE Transactions on Robotics and Automation, Volume 17, Issue 6, 947-951, 2001.
12. E. Fiorelli, et al., *Multi-AUV Control and Adaptive Sampling in Monterey Bay*. IEEE/OES Autonomous Underwater Vehicles, 134-147, 2004.
13. D. B. Edwards, et al., *A leader-follower algorithm for multiple AUV formations*. IEEE/OES Autonomous Underwater Vehicles, 40-46, 2004.
14. J.M. Soares, et al., *Joint ASV/AUV range-based formation control: Theory and experimental results*. IEEE International Conference on Robotics and Automation, 5579-5585, 2013.
15. M. Benjamin, H. Schmidt, P. Newman, J. Leonard, *Nested Autonomy for Unmanned Marine Vehicles with MOOS-IvP*. Journal of Field Robotics, Volume 27, Issue 6, 834-875, 2010.
16. O. Sorkine, *Least-Squares Rigid Motion Using SVD*. https://igl.ethz.ch/projects/ARAP/svd_rot.pdf, 2007, accessed 13 June 2015.
17. P.J. Haley, P.F.J. Lermusiaux, *Multiscale two-way embedding schemes for free-surface primitive equations in the "Multidisciplinary Simulation, Estimation and Assimilation System"*. Ocean Dynamics, Volume 60, Issue 6, 1497-1537, 2010.
18. A. Caffaz, et al., *The Hybrid Glider/AUV Folaga*. Robotics & Automation Magazine, Volume 17, Issue 1, 31-44, 2010.